Substitution of Membrane-Embedded Aspartic Acids in Bacteriorhodopsin Causes Specific Changes in Different Steps of the Photochemical Cycle†

Lawrence J. Stern,‡,§ Patrick L. Ahl,‖,⊥ Thomas Marti,‡ Tatsushi Mogi,‡,# Mireia Duñach,⊥ Stuart Berkowitz,⊥ Kenneth J. Rothschild,⊥ and H. Gobind Khorana*,‡

Departments of Chemistry and Biology, Massachusetts Institute of Technology, 77 Massachusetts Avenue, Cambridge, Massachusetts 02139, and Department of Physics, Boston University, Boston, Massachusetts 02215

Received May 15, 1989; Revised Manuscript Received August 3, 1989

ABSTRACT: Millisecond photocycle kinetics were measured at room temperature for 13 site-specific bacteriorhodopsin mutants in which single aspartic acid residues were replaced by asparagine, glutamic acid, or alanine. Replacement of aspartic acid residues expected to be within the membrane-embedded region of the protein (Asp-85, -96, -115, or -212) produced large alterations in the photocycle. Substitution of Asp-85 or Asp-212 by Asn altered or blocked formation of the M_{410} photointermediate. Substitution of these two residues by Glu decreased the amount of M_{410} formed. Substitutions of Asp-96 slowed the decay rate of the M_{410} photointermediate, and substitutions of Asp-115 slowed the decay rate of the O_{640} photointermediate. Corresponding substitutions of aspartic acid residues expected to be in cytoplasmic loop regions of the protein (Asp-36, -38, -102, or -104) resulted in little or no alteration of the photocycle. Our results indicate that the defects in proton pumping which we have previously observed upon substitution of Asp-85, Asp-96, Asp-115, and Asp-212 [Mogi, T., Stern, L. J., Marti, T., Chao, B. H., & Khorana, H. G. (1988) *Proc. Natl. Acad. Sci. U.S.A. 85*, 4148–4152] are closely coupled to alterations in the photocycle. The photocycle alterations observed in these mutants are discussed in relation to the functional roles of specific aspartic acid residues at different stages of the bacteriorhodopsin photocycle and the proton pumping mechanism.

Bacteriorhodopsin is a photosynthetic integral membrane protein found in the purple membrane patches of the archaebacterium *Halobacterium halobium*. It utilizes the energy of visible light to pump protons across the membrane against an electrochemical gradient. Bacteriorhodopsin is one of the simplest and most intensively studied ion pumps [for a review see Stoeckenius and Bogomolni (1982)], and yet the basic mechanism of light-driven proton transport is not understood in detail. Bacteriorhodopsin consists of a 248-residue apoprotein (Khorana et al., 1979) and an *all-trans*-retinal chromophore, which is covalently attached to Lys-216 via a protonated Schiff base (Huang et al., 1982; Rothschild et al., 1982). The protein is folded into seven transmembrane α-helices that surround the chromophore (Henderson & Unwin, 1975; Henderson et al., 1986; Heyn et al., 1988). Absorption of a photon causes isomerization of the chromophore to the 13-cis form and initiates the bacteriorhodopsin photocycle. During the photocycle, light-adapted bacteriorhodopsin (BR_{570}) transforms through at least five intermediate states, with lifetimes of 10^{-6}–10^{-2} s (Lozier et al., 1975):

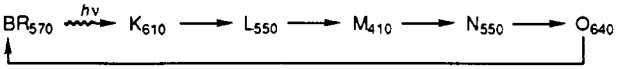

The dark-adapted form of bacteriorhodopsin has a distinct photocycle (Sperling et al., 1977; Iwasa et al., 1981). Additional pathways and intermediates may be required to describe the photocycle under all conditions (Nagle et al., 1982; Xie et al., 1987; Kouyama et al., 1988; Diller & Stockburger, 1988; Dancshazy et al., 1986; Drachev et al., 1987). The M_{410} intermediate is particularly important, as it contains a deprotonated Schiff base (Lewis et al., 1974). Approximately concurrent with the release of a proton from the Schiff base during M_{410} formation, a proton is released from the extracellular side of the membrane (Lozier et al., 1976). Proton uptake from the cytoplasmic side occurs later in the photocycle (Drachev et al., 1987; Kouyama et al., 1988). While there is a substantial body of information on the state of the chromophore at all steps of the photocycle (Smith et al., 1985), much less is known about the events in the protein that couple chromophore isomerization to transmembrane proton pumping.

To investigate the roles of individual amino acid residues in the proton pumping mechanism of bacteriorhodopsin, we have replaced a number of residues throughout the protein by the techniques of site-specific mutagenesis (Khorana, 1988; Hackett et al., 1987; Mogi et al., 1987, 1988; Stern & Khorana, 1989). Certain aspartic acid residues in particular seem to be important in the proton pumping mechanism (Mogi et al., 1988). Substitution of Asp-85, Asp-96, or Asp-212 severely reduced proton pumping activity, and substitution of Asp-115 also had a significant effect. Substitutions of aspartic acid residues expected to be outside the membrane bilayer in the

† Supported by grants from the National Institutes of Health (GM28289-09 and AI11479) and from the Office of Naval Research, Department of the Navy (N00014-82-K-0668) to H.G.K.; grants from the Office of Naval Research (N0014-88-K-0464) and the National Science Foundation (DMB-8806007) to K.J.R.; and a postdoctoral fellowship from the American Heart Association Massachusetts Affiliate to P.L.A. L.J.S. is a NIH predoctoral trainee, Th.M. is the recipient of a postdoctoral fellowship from the Swiss National Science Foundation, and M.D. is the recipient of a postdoctoral fellowship from the Spanish Government. This is Paper 12 in the series "Structure–Function Studies on Bacteriorhodopsin". Paper 11 is Flitsch and Khorana (1989).

* To whom correspondence should be addressed.

‡ Massachusetts Institute of Technology.

§ Present address: Department of Biochemistry and Molecular Biology, Harvard University, Cambridge, MA 02138.

‖ Present address: Department of Pathology and Laboratory of Medicine, Hahnemann University, Philadelphia, PA 19102.

⊥ Boston University.

Present address: Department of Biology, Faculty of Science, University of Tokyo, Hongo, Tokyo 113, Japan.

0006-2960/89/0428-10035$01.50/0

current structural model (Figure 1) had no effect on proton pumping activity.

In this study we have examined the effects of 13 aspartic acid substitutions on the bacteriorhodopsin photocycle. The results reported below show that replacement of aspartic acid residues that are buried within the membrane (positions 85, 96, 115, and 212) caused alterations in the photocycle. Notably, bacteriorhodopsin mutants with Asp → Asn substitutions at either position 85 or 212 altered the formation of an M-like[1] intermediate. Substitution of Asp-96 by Asn significantly slowed the decay rate of the M photointermediate in a pH-dependent manner. Substitution of Asp-115 altered the kinetics of the O intermediate. In contrast, Asp → Asn substitutions of aspartic acid residues located in cytoplasmic loop regions of the protein exhibited only minimal alterations of the photocycle.

Experimental Methods

Preparation of Mutant Bacteriorhodopsin Proteins. The construction of bacteriorhodopsin genes carrying single Asp → Asn, Asp → Glu, or Asp → Ala substitutions, and their expression in *Escherichia coli*, have been previously described (Mogi et al., 1988). Apoproteins were purified by solvent extraction and ion-exchange chromatography as previously described (Braiman et al., 1987) and regenerated with *all-trans*-retinal and polar lipids from *H. halobium* (Bayley et al., 1982) essentially as described (Popot et al., 1987). This preparation provides bacteriorhodopsin reconstituted in small unilamellar lipid vesicles (diameter <1000 Å) with a lipid:protein ratio of 1:1 (w/w). Absorption spectra of these vesicles were obtained with a Perkin-Elmer Lambda-7 UV–visible spectrophotometer, equipped with a light-scattering accessory. The vesicles were concentrated by centrifugation and resuspended at a bacteriorhodopsin concentration of 50–100 μM in 0.15 M KCl, 0.05 M potassium phosphate, and 0.025% NaN_3, pH 6.0. Unless noted, all experiments were performed at pH 6.0, where the regeneration yield (Liao et al., 1983; Popot et al., 1987) and protein stability (C. Brouillette, personal communication) are maximal.

Flash Spectroscopy. Photoreactions of the mutant proteins were measured in the millisecond time regime at 23 ± 1 °C, with a flash kinetic spectrophotometer of our own design (Ahl et al., 1989). For most experiments, the sample was held in a 1 mm × 1 mm (i.d.) glass cuvette, and the actinic source was from a home built dye laser (Ahl et al., 1989), which was pumped by a 250-kW N_2 laser (Cooper LaserSonics, Model UV-12, Santa Clara, CA). The coumarin 540A dye (540-nm emission, Exciton Chemical Inc., Dayton, OH) used for these experiments produced 0.2–0.3 mJ/flash at the sample, with a flash duration of 10–15 ns. The sample was flashed at a repetition rate of 1 or 2 Hz, and 500–2000 transients were averaged for each experiment.

Photocycle kinetics as a function of pH were measured with the same basic system adapted to 1 cm × 1 cm cuvettes. This allowed pH measurement and adjustment of the mutant samples within the cuvette. The sample was diluted 10-fold in the same buffer, and the pH was adjusted with microliter aliquots of 0.5 M HCl or 0.5 M NaOH. The actinic flash was provided by a Xe flashlamp (EG&G, Model FXP855, Salem, MA), filtered by a 520 nm long pass filter, and focused on the sample. The flashlamp intensity was approximately 2 mJ/flash, with a flash duration of about 20 μs. For each experiment, 50–100 transients were collected at a repetition rate of 0.1 Hz.

The actinic beams were oriented at right angles to the measuring beam. Intensity changes after an actinic flash were measured at various wavelengths (Ahl et al., 1989). The photomultiplier was protected from the actinic sources by narrow band interference filters. At 570 nm the interference filters did not completely block scattered laser illumination. To monitor any deterioration of the sample caused by repeated exposure to actinic flashes, kinetic traces at 570 nm were periodically obtained during the course of a series of measurements on a particular sample. If any significant alterations were observed in the 570-nm response, the entire series was repeated on a fresh sample, and the number of transients was reduced to minimize exposure to the actinic source.

Flash-induced visible difference spectra were obtained by using an optical multichannel analyzer and frequency-doubled Nd-YAG pulsed laser (80 mJ/flash at 532 nm) system that will be described in detail elsewhere (M. Duñach, S. Berkowitz, T. Mogi, T. Marti, H. G. Khorana, and K. J. Rothschild, unpublished results). Measurements were made at room temperature in a quartz cuvette at 4-nm resolution by using a signal acquisition window of 10 μs and signal averaged over 400 scans. The laser flash frequency was 5 Hz.

Data Analysis. The intensity changes were converted to absorbance changes by using

$$\Delta A(t) = -\log [(\Delta I(t)/I) + 1]$$

where I is the intensity of the measuring beam before the flash and $\Delta I(t)$ are the intensity changes as a function of time after the flash. Kinetic parameters for the absorbance changes at $t > 0.5$ ms were obtained by fitting the traces to multiexponential decay equations

$$\Delta A(t) = \sum_{n=1}^{p} A_n \exp(-t/\tau_n)$$

where p is the number of kinetic phases in the equation and A_n and $1/\tau_n$ are exponential constants. Absorbance traces were fit to a series of exponential equations with $p = 1$–3 by using a nonlinear least-squares regression algorithm (program 360D13.6.003; Triangle University Computation Center, Research Triangle Park, NC, and RS/1, BBN Software, Cambridge, MA). Goodness of fit was estimated by comparing the ratio of the χ^2 of the exponential fit to the χ^2 of a straight line fit to the preflash base line (Bevington, 1969). This ratio was usually around 1 and always less than 4.

Results

The locations of aspartic acid residues in bacteriorhodopsin that were investigated are indicated in Figure 1. The visible λ_{max} of mutant proteins, after reconstitution into *H. halobium* lipid vesicles, are shown in Table I. Asp-85→Asn, Asp-85→Glu, and Asp-212→Glu exhibited red-shifted chromophores relative to the wild-type protein, and Asp-115→Asn, Asp-115→Glu, Asp-212→Asn, and Asp-212→Ala exhibited blue shifts. Similar chromophore alterations were previously observed for these mutants in lipid/detergent micelles (Mogi et al., 1988).

Wild-Type Bacteriorhodopsin. Flash-induced absorbance changes at 410, 570, and 640 nm for wild-type bacteriorhodopsin at pH 6.0 are displayed in Figure 2A. These traces are identical with those observed with the native protein from *H. halobium* which has been reconstituted into lipid vesicles and are similar to those obtained with the native purple membrane (Ahl et al., 1989). The absorbance changes at 410,

[1] We omit the subscripts conventionally used to indicate the absorption maxima of bacteriorhodopsin photointermediates, in discussion of the mutant photocycles, since the absorption bands of the photointermediates may be shifted.

Table I: Kinetic Parameters of the Flash-Induced Absorbance Changes of Aspartic Acid Mutants at pH 6[a]

mutant	λ_{max} (nm)	410 nm		570 nm	
		τ_1[b] (ms)	τ_2[b] (ms)	τ_1[b] (ms)	τ_2[b] (ms)
wild type	558	4.8 (100)		4.3 (84)	20 (16)
Asp-36→Asn	556	3.1 (80)	13 (20)	4.9 (87)	20 (13)
Asp-38→Asn	562	5.8 (81)	26 (19)	6.7 (84)	33 (16)
Asp-85→Asn	580	ND[c]	ND[c]	2.9[d] (80)	64 (20)
Asp-85→Glu	607	6.1 (73)	45 (27)	6.9 (63)	48 (37)
Asp-96→Asn	567	5.6 (100)		5.4 (71)	36 (29)
Asp-96→Glu	560		30 (100)		37 (100)
Asp-102→Asn	557	8.8 (100)		4.7 (69)	21 (31)
Asp-104→Asn	560	6.7 (100)		6.9 (82)	26 (18)
Asp-115→Asn	546	2.1 (60)	15 (40)	3.8 (65)	45 (35)
Asp-115→Glu	531	14 (37)	76 (63)	11 (46)	77 (54)
Asp-212→Asn	534	ND[c]	ND[c]	0.8[d] (94)	125 (6)
Asp-212→Glu	576		65 (100)		63 (100)
Asp-212→Ala	520	5.5 (77)	31 (23)	8.8 (72)	40 (28)

[a] Kinetic traces of the sort shown in Figures 2, 3, and 5 were obtained with various time bases and were fit to exponential models (see Experimental Methods). [b] Exponential decay time. Values in parentheses indicate the percentage of the total absorbance change represented by that decay time. [c] No absorbance change was detected (detection limit 10^{-4} AU or <0.3% of the wild-type signal). [d] Exponential decay times for these components are less certain due to interference from scattered actinic illumination.

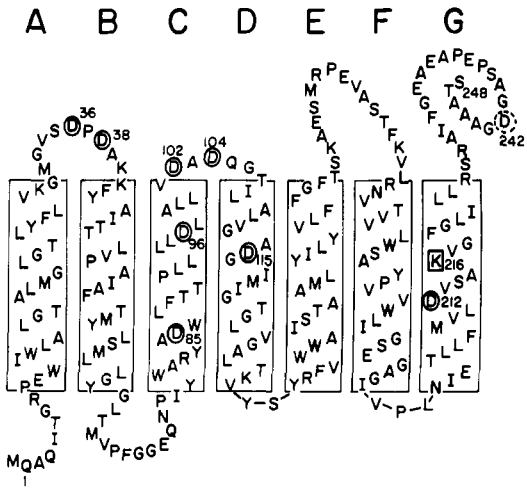

FIGURE 1: Aspartic acid mutations of bacteriorhodopsin. Residues investigated in the present work are indicated on a secondary structure model for bacteriorhodopsin. Aspartic acid residues that were individually changed to asparagine are indicated by ovals. Asp-242, indicated by a dotted oval, was not replaced: it has previously been shown to be unimportant for proton pumping or photocycling activity (Liao & Khorana, 1984; Ovchinnikov et al., 1986). Membrane-buried residues Asp-85, Asp-96, Asp-115, and Asp-212 were also substituted by glutamic acid, and Asp-212 was also substituted by alanine. Lys-216, the site of attachment of the retinal chromophore, is boxed.

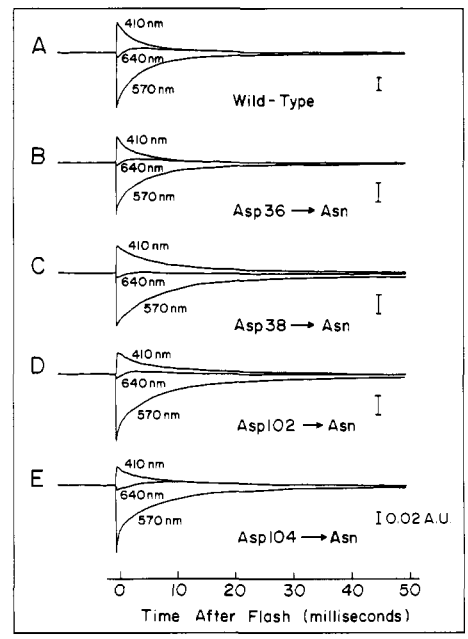

FIGURE 2: Flash-induced absorbance changes of wild-type bacteriorhodopsin, Asp-36→Asn, Asp-38→Asn, Asp-102→Asn, and Asp-104→Asn. Kinetic absorbance changes were measured at 410, 570, and 640 nm, as indicated, at pH 6.0 and at 23 ± 1 °C. The sample was flashed with a 540-nm laser pulse at time = 0 s. Vertical bars at right represent 0.02 AU. The horizontal scale is the same for all traces. The measured absorbance of each sample at 570 nm is indicated in parentheses below. (A) Wild-type bacteriorhodopsin (1.0); (B) Asp-36→Asn (0.5); (C) Asp-38→Asn (0.7); (D) Asp-102→Asn (0.7); (E) Asp-104→Asn (1.2).

570, and 640 nm are described in more detail below. The large positive signal at 410 nm is due to the formation and decay of the M intermediate. At this resolution (80 μs/point) the formation kinetics of the M intermediate cannot be accurately determined. The decay kinetics of the 410-nm trace were fit to an exponential model (see Experimental Methods). The trace is well described by a single-exponential decay, with an exponential time constant τ = 4.8 ms (Table I). The large negative signal at 570 nm indicates depletion of the BR state as the intermediates of the photocycle are formed. The return of the 570-nm absorbance to the preflash base line indicates the repopulation of the BR state and completion of the photocycle. Kinetic parameters for the wild-type 570-nm absorbance change are shown in Table I. The trace is best fit by a two-exponential model, with a fast component (85% of the total 570-nm absorbance change) that has an exponential decay time τ = 4.3 ms, close to the τ for M decay, and a slower phase (15%) with τ = 20 ms. Absorbance changes at 640 nm are due to the rise and decay of the O intermediate, with a small contribution from the BR return, since the BR state has significant absorption at 640 nm. After subtraction of the residual BR signal, the 640-nm trace can be accurately described by a two-exponential rate equation. The rise phase has τ = 1.3 ms, and the decay phase has τ = 7.8 ms.

Substitutions of Aspartic Acid Residues in the Cytoplasmic Loops. Flash-induced absorbance changes at 410, 570, and 640 nm for Asp-36→Asn, Asp-38→Asn, Asp-102→Asn, and Asp-104→Asn are shown in Figure 2B–E, respectively. All of these mutants exhibited photocycles qualitatively like those of wild-type bacteriorhodopsin. The rise and decay times, and the relative amplitudes of the BR, M, and O signals, are similar to those exhibited by the wild-type protein. The relative amplitudes of the fast and slow kinetic components of the M and BR traces are somewhat perturbed in some of these mutants (Table I). However, it is clear that these mutations have not

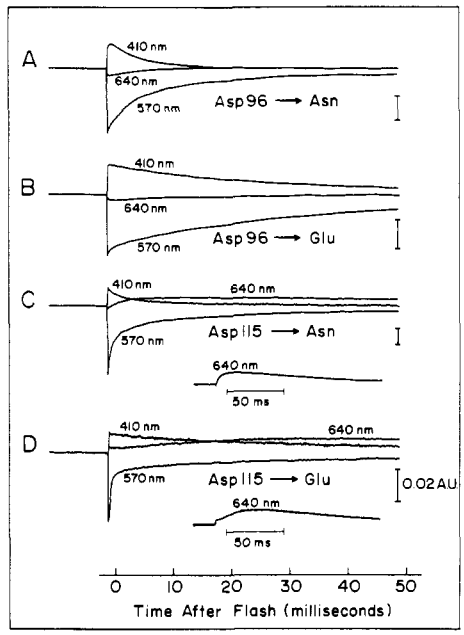

FIGURE 3: Flash-induced absorbance changes of Asp-96→Asn, Asp-96→Glu, Asp-115→Asn, and Asp-115→Glu. See legend to Figure 2 for details. (A) Asp-96→Asn (0.6); (B) Asp-96→Glu (0.6); (C) Asp-115→Asn (0.2); (D) Asp-115→Glu (0.3). The insets in panels C and D show the 640-nm absorbance traces on a longer time scale.

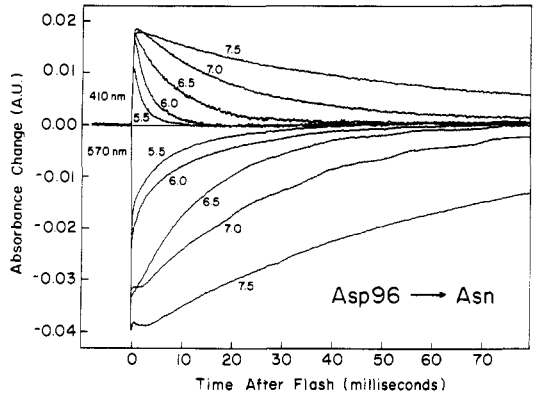

FIGURE 4: pH dependence of flash-induced absorbance changes at 410 and 570 nm of Asp-96→Asn. (Top) Absorbance changes at 410 nm; (bottom) absorbance changes at 570 nm. Kinetic traces were obtained at pH 5.5–7.5 as indicated. This sample had A_{570} = 0.5.

significantly altered the overall photocycle.

Asn and Glu Substitutions of Asp-96. Flash-induced absorbance changes for the Asp-96→Asn substitution are shown in Figure 3A. The amplitudes of the 410- and 570-nm traces are similar to those of the wild-type, but no absorbance change at 640 nm is observed above the residual BR signal. At pH 6.0, kinetic parameters for the absorbance change at 410 and 570 nm are similar to those of the wild-type (Table I). However, the photocycle of this mutant is extremely sensitive to pH. Flash-induced absorbance changes at 410 and 570 nm for Asp-96→Asn as a function of pH are shown in Figure 4. As the pH is increased from 5.5 to 7.5, both the 410- and 570-nm kinetics are slowed more than 10-fold. The amplitudes of the absorbance changes at these wavelengths are essentially constant over this pH range. At pH 7.5, τ = 70 ms for both the 410- and 570-nm absorbance changes.

Flash-induced absorbance changes for Asp-96→Glu (pH 6.0) are shown in Figure 3B. Both the 410- and 570-nm kinetics are significantly slowed by this substitution (Table I). As with Asp-96→Asn, no absorbance increase at 640 nm is observed above the residual bR signal. The amplitudes of

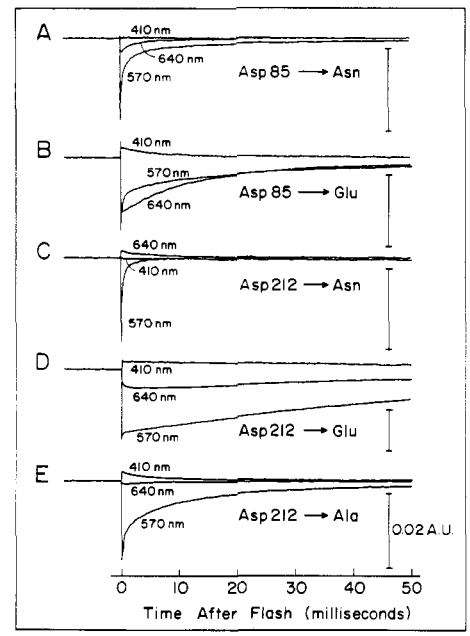

FIGURE 5: Flash-induced absorbance changes of Asp-85→Asn, Asp-85→Glu, Asp-212→Asn, Asp-212→Glu, and Asp-212→Ala. See legend to Figure 2 for details. (A) Asp-85→Asn (0.6); (B) Asp-85→Glu (0.5); (C) Asp-212→Asn (0.7); (D) Asp-212→Glu (0.5); (E) Asp-212→Ala (0.5).

the 410- and 570-nm absorbance changes are comparable to those of the wild type.

Asn and Glu Substitutions of Asp-115. Flash-induced absorbance changes for Asp-115→Asn are shown in Figure 3C. The 410- and 570-nm absorbance changes have kinetics similar to those of the wild type, except that there is an increased proportion of the slow decay components (Table I). The amplitude of the absorbance change at 410 nm is significantly reduced relative to that at 570 nm. The major alteration in this mutant is seen at 640 nm. The 640-nm signal shows a rise (τ = 4 ms) with kinetics similar to that of the wild type, but the decay of this signal is very slow (τ = 102 ms), more than 10-fold slower than the decay of the wild-type 640-nm signal.

The Asp-115→Glu photocycle is even more perturbed (Figure 3D). The 410-nm absorbance change is relatively small and has a very slow decay. The major kinetic component of the 410-nm absorbance decay has τ = 76 ms (Table I). Most of the 570-nm absorbance change decays very quickly (τ < 1 ms). The remainder of the 570-nm signal (26%) corresponds in amplitude and kinetics to the 410-nm signal. The 640-nm signal exhibits large alterations in both the rise and decay kinetics. The rise of the 640-nm absorbance change has τ = 27 ms, 20-fold slower than the rise of the wild-type 640-nm signal. The 640-nm decay is also slow (τ = 60 ms), as with the Asp-115→Asn substitution.

Asn and Glu Substitutions of Asp-85. Flash-induced absorbance changes for the Asp-85→Asn substitution are shown in Figure 5A. No significant absorbance increase was observed at 410 nm. The noise level in this trace is 8.2×10^{-5} AU,[2] indicating that any undetected 410-nm rise represents less than 0.3% of the expected signal. The 570-nm absorbance decrease was also significantly reduced relative to the wild-type signal. No 640-nm absorbance increase was observed.

To further characterize this highly perturbed photoresponse, flash-induced difference spectra were measured over the visible wavelength region (350–700 nm) at various times after a laser

[2] Abbreviations: AU, absorbance unit; FTIR, Fourier transform infrared.

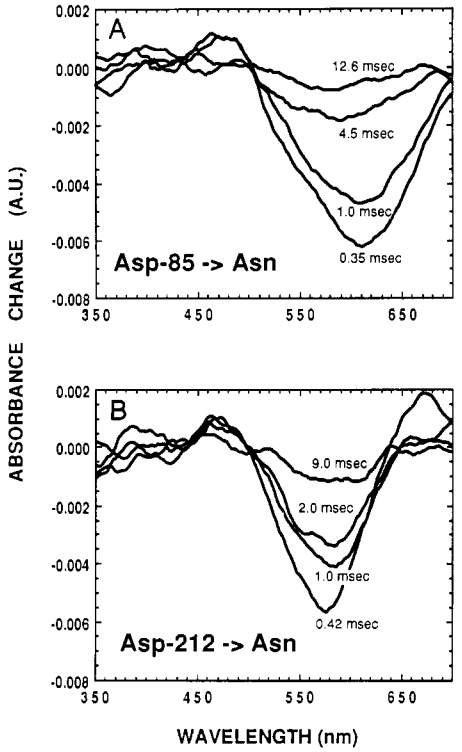

FIGURE 6: Flash-induced difference spectra of Asp-85→Asn and Asp-212→Asn. Spectra were measured at pH 6.0 at ambient temperature, at the indicated times after a laser flash (10-μs acquisition window). Light-induced difference spectra were calculated by subtraction of spectra obtained alternately with and without laser illumination. Values in parentheses indicate the measured absorbance for each sample. (A) Asp-85→Asn (0.5, 580 nm); (B) Asp-212→Asn (0.5, 534 nm).

flash (Figure 6A). The major features of these spectra are a depletion band centered near 610 nm and an absorbance increase near 470 nm. Thus, the absorbance decrease at 570 and 640 nm seen in Figure 6A is due to the depletion of a red-shifted species with λ_{max} near 610 nm. No evidence for an M-like intermediate is seen in this time regime. The photocycle of this mutant was also studied as a function of pH. As the pH was raised above 7, a small positive absorbance change at 410 nm was observed, which increased with increasing pH. Figure 7 shows the 410-nm signal observed at pH 8 for Asp-85→Asn, on a greatly expanded scale. The amplitude of this absorbance change is about 5% of that observed for the wild type. Kinetic analysis revealed a rise component with τ = 3 ms and a decay component with τ = 5 ms. The rise of the 410-nm absorbance change at pH 8.0 is thus more than 30-fold slower than that of the wild-type signal, which is also shown in Figure 7 for comparison. The decay kinetics of this signal are similar to those of the wild type. At pH 9.0, a similar 410-nm absorbance increase was observed, with a slightly larger amplitude and a slower decay. No large alterations in the 570-nm absorbance changes were observed in the range pH 6.0–9.0.

The kinetic traces for Asp-85→Glu are shown in Figure 5B. A positive 410-nm absorbance change is seen for this mutant, but its amplitude is reduced to 30% of the wild-type signal, and its decay kinetics are slightly slower than those of the wild type (Table I). The 570-nm absorbance change has two kinetic components which correspond in amplitude and kinetics to those seen in the 410-nm signal. At 640 nm, Asp-85→Glu shows a large negative absorbance change, with kinetics similar to those of the slow phase of the 570-nm trace. The photocycle of Asp-85→Glu was also investigated in the pH range 6–9 (data not shown). Over this range the 410-nm amplitude

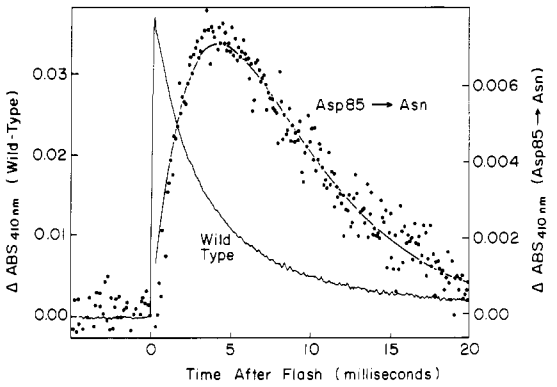

FIGURE 7: Flash-induced absorbance changes at 410 nm of Asp-85→Asn at pH 8.0. Individual data points are indicated for Asp-85→Asn; the smooth curve through them indicates a two-exponential kinetic model. Data points for the wild-type trace are connected by straight segments. Note the different absorbance scales for the two traces. The absorbance scale on the right refers to the Asp-85→Asn trace. The absorbance scale on the left refers to the wild-type trace. The 570-nm absorbance of both of these samples was 0.9.

increased to 50% of the wild-type level, and the kinetics became more like those of the wild type. As the pH was increased above 9, a species with λ_{max} of 460 nm was formed. The 460-nm species exhibited a highly perturbed photocycle with flash-induced changes that persisted for >1 s.

Asn, Glu, and Ala Substitutions of Asp-212. The flash-induced absorbance changes at 410, 570, and 640 nm for Asp-212→Asn are shown in Figure 5C. No absorbance increase at 410 nm was observed. The 570-nm signal exhibits a fast decay (τ < 1 ms). An absorbance increase at 640 nm was observed. The rise time of this signal is less than the 10-μs resolution of our instrument. In addition, there are slow decay components for both 570- and 640-nm decays. These results indicate that the photocycle of this mutant is highly perturbed. Absorbance changes obtained at a flash repetition rate of 0.1–10 Hz showed the same characteristics.

To further characterize this photoresponse, flash-induced difference spectra were obtained throughout the visible-wavelength region (Figure 6B). The major feature of these spectra is a large negative peak centered near 580 nm; a positive signal centered near 660 nm is also observed. As with the Asp-85→Asn substitution, no absorbance increase consistent with the formation of an M-like intermediate is observed. The photocycle of Asp-212→Asn was also studied as a function of pH, over the pH range 6–9 (data not shown). No significant absorbance increase at 410 nm was observed at any pH. The 570-nm absorbance change remained essentially constant over this range.

Flash-induced absorbance changes for Asp-212→Glu are shown in Figure 5D. Absorbance changes at 410 and 570 nm characteristic of the formation and decay of M and the return to the BR state were observed. However, the 410-nm absorbance increase is small compared to the 570-nm decrease, and the decay rates of both absorbance changes were extremely slow (Table I). No 640-nm rise is observed over the residual BR signal seen at this wavelength. The signals remained essentially constant over the pH range 6–8, except that the 410-nm decay rate became even slower at higher pH.

Flash-induced absorbance changes for Asp-212→Ala are shown in Figure 5E. This mutant was sensitive to light and exhibited some irreversible bleaching upon repeated exposure to actinic flashes. A small absorbance increase at 410 nm was observed, with 18% of the expected amplitude. Kinetic analysis (Table I) revealed one decay component with a τ value similar to that of the wild type and a smaller component with much

larger decay. At 570 nm, both fast and slow components were observed (Table I). No absorbance increase was observed at 640 nm.

Discussion

We have previously described the construction of bacteriorhodopsin mutants in which aspartic acid residues were replaced by asparagine, glutamic acid, or alanine (Mogi et al., 1988). Substitution of Asp-85, Asp-96, or Asp-212 led to dramatic decreases in proton pumping activity, while substitution of Asp-115 also had a significant effect (Mogi et al., 1988). To understand in more detail the cause of the reduced proton pumping activity seen with these mutants, and to further investigate the roles of the aspartic acid residues in bacteriorhodopsin, we have studied the photocycles of 13 aspartic acid mutants by flash spectroscopy. The amino acid substitutions caused specific alterations at different steps in the photocycle. The effects of these substitutions are discussed below, in relation to the role of each aspartic acid residue in the photocycle and in the proton pumping mechanism.

Asp-36, -38, -102, and -104. The aspartic acids at positions 36, 38, 102, and 104 are expected to be located in cytoplasmic loop regions of bacteriorhodopsin (Figure 1). Mutants containing asparagine substitutions at each of these positions were previously shown to have full light-dependent proton pumping activity (Mogi et al., 1988). Here we have shown that they also exhibit normal photocycles. Together these results show that the carboxyl groups present at these positions have no important role in the photocycle or in the proton pumping mechanism. Four other carboxylate residues, Glu-232, Glu-234, Glu-237, and Asp-242, are located near the C-terminus of bacteriorhodopsin on a segment exposed to the cytoplasmic medium (Gerber et al., 1977). This segment can be removed by proteolysis, without reducing proton pumping or photocycling activity (Liao & Khorana, 1984; Ovchinnikov et al., 1986). The remaining cytoplasmic carboxylate residues, Glu-161 and Glu-166, are also unimportant for proton pumping (L.J.S. and H.G.K., unpublished results). Thus none of the 10 cytoplasmic carboxylate residues are involved in any significant way in the proton pumping mechanism. Collectively they provide a highly negative surface charge, which may play some other role, for example, in membrane insertion.

Asp-85. The results presented here show that replacement of Asp-85 by asparagine severely reduces or eliminates the ability to populate an M_{410}-like photointermediate. The 350 μs flash induced difference spectrum of Asp-85→Asn, obtained at pH 6 (Figure 6A), indicates that the major photoactive species is red-shifted relative to the wild type and gives rise to a 480-nm absorbing intermediate. These photoreactions are similar to those of "blue membrane" (M.D. and K.J.R., unpublished results; Mowery et al., 1979). As the pH is raised above 7, a small increase at 410 nm is observed, consistent with the very slow formation of an M-like photointermediate. At pH 8, formation kinetics of this signal are more than 30-fold slower than the wild-type signal, although the decay kinetics are normal (Figure 7). Since the rise and decay times of this M-like intermediate are similar, the observed amplitudes of the M signal are quite small. Substitution of Asp-85 by glutamic acid restores the ability to form an M-like intermediate. The alterations that are observed with Asp-85→Glu [broadened chromophore band (Mogi et al., 1988), red-shifted λ_{max}, reduced 410-nm amplitude, and large absorbance change at 640 nm] could be due to the presence of some amount of a red-shifted species, similar to that observed with Asp-85→Asn.

These results suggest that a carboxylic acid at position 85 is required for formation of the M intermediate and efficient deprotonation of the Schiff base. Asp-85 may be the primary acceptor of the Schiff base proton during M formation. Fourier transform infrared (FTIR)[2] experiments have demonstrated that Asp-85 protonates during the formation of M and suggested that Asp-85 may act as the acceptor of the Schiff base proton (Braiman et al., 1988). Here we have demonstrated that blocking this protonation, by replacement of Asp-85 with asparagine, also blocks M formation. The greatly slowed deprotonation observed for Asp-85→Asn at high pH probably represents the inefficient deprotonation of the Schiff base by another residue or by the bulk aqueous phase.

Asp-96. Mutants in which Asp-96 was replaced by either asparagine or glutamic acid exhibited a 410-nm signal with the same amplitude as that of the wild-type protein, indicating that both of these mutants are capable of forming an M-like intermediate. However, substitutions at this position altered the rate of M decay. Asp-96→Glu exhibited M decay kinetics 6 times slower than those observed with the wild-type protein. Asp-96→Asn exhibited normal kinetics at pH 6, but the rate of M decay decreased sharply with increasing pH (Figure 4). Thus, substitution of Asp-96 can interfere with the mechanism of Schiff base reprotonation.

Previously, substitution of Asp-96 was shown to decrease the proton pumping efficiency (Mogi et al., 1988), specifically by slowing the rate of uptake of protons from the aqueous medium (Marinetti et al., 1989). Both the overall pumping efficiency for Asp-96→Asn and the rate of proton uptake decrease as the pH increases, in parallel to the changes in the Schiff base reprotonation rate (Holz et al., 1989). Taken together, these results suggest that Asp-96 facilitates the transfer of a proton from the cytoplasmic medium to the deprotonated Schiff base. However, the carboxylate of Asp-96 cannot be the obligate donor of a proton to the Schiff base, as efficient Schiff base reprotonation is observed at low pH for Asp-96→Asn. Asp-96 may function as a proton relay in the pathway that serves to reprotonate the Schiff base with a proton derived from the cytoplasmic medium (Braiman et al., 1988). Other pathways for reprotonation of the Schiff base that exclude Asp-96 must exist and are apparently as efficient at low pH.

Asp-115. Replacements of Asp-115 also caused alterations in the photocycle. Substitution of Asp-115 by glutamic acid caused more severe pertubations of the photocycle than substitution by asparagine. This parallels the effects of these substitutions on the chromophore λ_{max}, proton pumping activity (Mogi et al., 1988) and quantum yield (Marinetti et al., 1989). Asparagine is thus a more conservative replacement for Asp-115 than glutamic acid. This is reasonable, since Asp-115 appears to remain in the un-ionized (protonated) form throughout the photocycle (Braiman et al., 1988).

Both Asp-115→Asn and Asp-115→Glu substitutions exhibited absorbance changes at 410 and 640 nm consistent with the formation of M and O photointermediates, but for both mutants the decay time of the 640 nm absorbing species was severely slowed. For Asp-115→Glu, the M decay rate is also slowed. In both cases, however, the 640-nm rise is coupled to the 410-nm decay. These results indicate that substitution of Asp-115 interferes with the O → BR conversion. This step is believed to involve a conformational relaxation of the protein around the reisomerized (all-trans) chromophore (Smith et al., 1983). The structural requirements at position 115 for efficient O → BR conversion are quite strict: Asp → Asn and Asp → Glu both cause large alterations in this step. Asp-

115→Glu and Asp-115→Asn both exhibit altered λ_{max} (Table I) and slowed chromophore regeneration (Mogi et al., 1988), also indicating a specific requirement for aspartic acid at position 115.

Asp-212. Substitutions at Asp-212 caused more complicated alterations in the photocycle than those observed for the other mutants. When Asp-212 is replaced by Asn, no absorbance change consistent with the formation of an M-like intermediate is observed at any time after the flash, over the pH range 6–9. A 660-nm absorbing species with a very fast rise and a slow decay was observed. These photoreactions are somewhat similar to those of the 13-cis component of dark-adapted bacteriorhodopsin (Sperling et al., 1977; Iwasa et al., 1981). Reversed λ_{max} shifts upon light–dark adaptation (L.J.S., H.G.K., and K.J.R., unpublished observations) and an increased 13-cis component in the FTIR low-temperature difference spectrum (M. Braiman and K.J.R., personal communication) have also been observed for Asp-212→Asn in reconstituted vesicles. This substitution may thus have shifted the usual chromophore all-trans ⇌ 13-cis equilibrium toward the 13-cis species. This complicates the use of this mutant for investigation of the role of Asp-212 in the usual all-trans photocycle. In other systems Asp-212→Asn has previously shown partial proton pumping activity (Mogi et al., 1988; Marinetti et al., 1989), suggesting that under some conditions the normal all-trans photocycle may be partially active.

Although no M-like photointermediate was observed for Asp-212→Asn under any conditions investigated, Asp-212→Ala was able to form a small amount of an M-like photointermediate that had relatively normal formation and decay kinetics (Figure 5E). We cannot therefore assign an obligatory role to the carboxylate of Asp-212 in the deprotonation or reprotonation reactions of the Schiff base required for M formation and decay. However, Asp-212 is clearly involved in specific interactions that control the stability and isomeric state of the chromophore.

Replacement of Asp-212 by glutamic acid also resulted in an altered photocycle. This substitution significantly lengthened the overall lifetime of the photocycle, due to a more than 10-fold decrease in the rate of M intermediate decay (Schiff base reprotonation). Asp-212→Glu was previously shown to exhibit slowed proton uptake kinetics (Marinetti et al., 1989). Thus, this substitution has an effect similar to that of substitutions at Asp-96. However, in this case, slowed M decay was observed over a large pH range. This slowing of the reprotonation rate for Asp-212→Glu may be due to an alteration of the normal protein–chromophore interactions near the Schiff base. Interestingly, a number of other single amino acid substitutions in bacteriorhodopsin significantly decreased the rate of Schiff base reprotonation. These include Asp-96→Asn (high pH), Asp-96→Glu and Asp-115→Glu, described above, Arg-227→Gln (Stern & Khorana, 1989), and to a lesser degree Tyr-185→Phe (Ahl et al., 1989) and Trp-137→Cys (L.J.S., unpublished observations). These residues are located in different helices and at different depths within the membrane. It is unlikely that they can all approach the Schiff base to directly participate in the reprotonation process. This suggests that some degree of conformational rearrangement involving residues throughout the protein must occur during the decay of the M intermediate. Such conformational changes have been previously proposed on other grounds (Draheim & Cassim, 1985; Hasselbacher et al., 1986; Fodor et al., 1988).

Summary

In conclusion, we have demonstrated that the defects in bacteriorhodopsin proton pumping previously observed upon substitutions of membrane-buried aspartic acid residues are accompanied by specific alterations of distinct steps in the photocycle. We were able to confirm a functional role for the carboxylate group of Asp-85 in the deprotonation of the Schiff base, as has been previously suggested on the basis of FTIR studies (Braiman et al., 1988). Asp-96 is involved in the reprotonation pathway, although its role is less clear. An aspartic acid at position 115 is required for efficient relaxation from the O state back to the BR resting state. Asp-212 is also involved in the reprotonation pathway and is required for stabilization and proper isomerization of the chromophore, probably due to a direct interaction with the Schiff base. Further insight into the roles of these residues can be provided by studies of proton transfers within the protein during the pumping cycle by use of FTIR spectroscopy and electrochemical measurements.

Acknowledgments

We thank Professor Uttam L. RajBhandary for suggestions and encouragement and Sriram Subramaniam for many helpful discussions during the course of this work. We also thank Maarten Heyn for a critical review of the manuscript.

Registry No. Asp, 56-84-8; H, 12408-02-5.

References

Ahl, P. L., Stern, L. J., Mogi, T., Khorana, H. G., & Rothschild, K. J. (1989) *Biochemisty* (preceding paper in this issue).

Bayley, H., Hojeberg, B., Huang, K.-S., Khorana, H. G., Liao, M.-J., Lind, C., & London, E. (1982) *Methods Enzymol. 88*, 74–81.

Bevington, P. R. (1969) in *Data Reduction and Error Analysis for the Physical Sciences*, McGraw-Hill, New York.

Braiman, M. S., Stern, L. J., Chao, B. H., & Khorana, H. G. (1987) *J. Biol. Chem. 262*, 9271–9276.

Braiman, M. S., Mogi, T., Marti, T., Stern, L. J., Khorana, H. G., & Rothschild, K. J. (1988) *Biochemistry 27*, 8516–8520.

Dancshazy, Z., Govindjee, R., Nelson, B., & Ebrey, T. G. (1986) *FEBS Lett. 209*, 44–48.

Diller, R., & Stockburger, M. (1988) *Biochemistry 27*, 7641–7651.

Drachev, L. A., Kaulen, A. D., Skulachev, V. P., & Zorina, V. V. (1987) *FEBS Lett. 226*, 139–144.

Drahein, J. E., & Cassim, J. Y. (1985) *Biophys. J. 47*, 497–507.

Flitsch, S. L., & Khorana, H. G. (1989) *Biochemistry 28*, 7800–7805.

Fodor, S. P. A., Ames, J. B., Gebhard, R., Van den Berg, E. M. M., Stoeckenius, W., Lugtenburg, J., & Mathies, R. A. (1988) *Biochemistry 27*, 7097–7101.

Gerber, G. E., Gray, C. P., Wildenauer, D., & Khorana, H. G. (1977) *Proc. Natl. Acad. Sci. U.S.A. 74*, 5426–5430.

Hackett, N. R., Stern, L. J., Chao, B. H., Kronis, K. A., & Khorana, H. G. (1987) *J. Biol. Chem. 262*, 9277–9284.

Hasselbacher, C. A., Preuss, D. K., & Dewey, T. G. (1986) *Biochemistry 25*, 668–676.

Henderson, R., & Unwin, P. N. T. (1975) *Nature 257*, 28–32.

Henderson, R., Baldwin, J. M., Downing, K. H., Lepault, J., & Zemlin, F. (1986) *Ultramicroscopy 19*, 147–178.

Heyn, M. P., Westerhausen, J., Wallat, I., & Seiff, F. (1988) *Proc. Natl. Acad. Sci. U.S.A. 85*, 2146–2150.

Holz, M., Drachev, L. A., Mogi, T., Otto, H., Kaulen, A. D., Heyn, M. P., Skulachev, V. P., & Khorana, H. G. (1989) *Proc. Natl. Acad. Sci. U.S.A. 86*, 2167–2171.

Huang, K.-S., Liao, M.-J., Gupta, C. M., Royal, N., Biemann, K., & Khorana, H. G. (1982) *J. Biol. Chem. 257*, 8596–8599.

Iwasa, T., Tokunaga, F., & Yoshizawa, T. (1981) *Photochem. Photobiol. 33*, 539–545.

Khorana, H. G. (1988) *J. Biol. Chem. 263*, 7439–7442.

Khorana, H. G., Gerber, G. E., Herlihy, W. C., Cray, C. P., Anderegg, R. J., Nihei, K., & Biemann, K. (1979) *Proc. Natl. Acad. Sci. U.S.A. 76*, 5046–5050.

Kouyama, T., Nasuda-Kouyama, A., Ikegami, A., Mathew, M. K., & Stoeckenius, W. (1988) *Biochemistry 27*, 5855–5863.

Lewis, A., Spoonhower, J., Bogomolni, R. A., Lozier, R. H., & Stoeckenius, W. (1974) *Proc. Natl. Acad. Sci. U.S.A. 71*, 4462–4466.

Liao, M.-J., & Khorana, H. G. (1984) *J. Biol. Chem. 259*, 4194–4199.

Liao, M.-J., London, E., & Khorana, H. G. (1983) *J. Biol. Chem. 258*, 9949–9955.

Lozier, R. H., Bogomolni, R. A., & Stoeckenius, W. (1975) *Biophys. J. 15*, 955–962.

Lozier, R. H., Niederberger, W., Bogomolni, R. A., Hwang, S.-H., & Stoeckenius, W. (1976) *Biochim. Biophys. Acta 440*, 545–556.

Marinetti, T., Subramaniam, S., Mogi, T., Marti, T., & Khorana, H. G. (1989) *Proc. Natl. Acad. Sci. U.S.A. 86*, 529–533.

Mogi, T., Stern, L. J., Hackett, N. R., & Khorana, H. G. (1987) *Proc. Natl. Acad. Sci. U.S.A. 84*, 5595–5599.

Mogi, T., Stern, L. J., Marti, T., Chao, B. H., & Khorana, H. G. (1988) *Proc. Natl. Acad. Sci. U.S.A. 85*, 4148–4152.

Mowery, P. C., Lozier, R. H., Chae, Q., Tseng, Y.-W., Taylor, M., & Stoeckenius, W. (1979) *Biochemistry 18*, 4100–4107.

Nagle, J. F., Parodi, L. A., & Lozier, R. H. (1982) *Biophys. J. 38*, 161–174.

Ovchinnikov, Yu. A., Abdulaev, N. G., Kiselev, A. V., Drachev, L. A., Kaulen, A. D., & Skulachev, V. P. (1986) *FEBS Lett. 194*, 16–20.

Popot, J.-L., Gerchman, S.-E., & Engelman, D. M. (1987) *J. Mol. Biol. 198*, 655–676.

Rothschild, K. J., Argade, P. V., Earnest, T. N., Huang, K.-S., London, E. W., Liao, M.-J., Bayley, H., Khorana, H. G., & Herzfeld, J. (1982) *J. Biol. Chem. 257*, 8592–8595.

Smith, S. O., Pardoen, J. A., Mulder, P. P. J., Curry, B., Lugtenburg, J., & Mathies, R. A. (1983) *Biochemistry 22*, 6141–6148.

Smith, S. O., Lugtenburg, J., & Mathies, R. A. (1985) *J. Membr. Biol. 85*, 95–109.

Sperling, W., Carl, P., Rafferty, C. N., & Dencher, N. A. (1977) *Biophys. Struct. Mech. 3*, 79–94.

Stern, L. J., & Khorana, H. G. (1989) *J. Biol. Chem. 264*, 14202–14208.

Stoeckenius, W., & Bogomolni, R. A. (1982) *Annu. Rev. Biochem. 52*, 587–616.

Xie, A. H., Nagle, J. F., & Lozier, R. H. (1987) *Biophys. J. 51*, 627–635.